CONSTITUTIVE MODEL OF PLASTIC STRAIN INDUCED PHENOMENA AT CRYOGENIC TEMPERATURES

Błażej Skoczeń

Cracow University of Technology, Institute of Applied Mechanics, Cracow, Poland
e-mail: blazej.skoczen@pk.edu.pl

FCC metals and alloys are frequently used in cryogenic applications, nearly down to the temperature of absolute zero, because of their excellent physical and mechanical properties, including ductility. These materials, often characterized by the Low Stacking Fault Energy (LSFE), undergo at low temperatures three distinct phenomena: Dynamic Strain Ageing (DSA), plastic strain induced transformation from the parent phase γ to the secondary phase α' and evolution of micro-damage. As all three phenomena lead to irreversible degradation of lattice and can accelerate the process of material failure, a combined constitutive description appears to be fundamental for the correct analysis of structures applied at very low temperatures. The constitutive model presented in the paper takes into account all the three phenomena as well as the relevant thermodynamic background.

Key words: constitutive behaviour, yield condition, phase transformation, voids and inclusions, cryogenic temperature

1. Introduction

FCC metals and alloys (such as copper, copper alloys or stainless steel) are often applied in cryogenic conditions, down to the temperature in the proximity of absolute zero, because of their remarkable properties including ductility. A broad class of these materials is characterized by the Low Stacking Fault Energy (LSFE). Therefore, they undergo both Dynamic Strain Ageing (DSA) and transformation from the parent phase γ to the secondary phase α' at extremely low temperatures. Both phenomena can be classified as material instabilities associated on one hand with an oscillatory mode of plastic flow (DSA effect) and, on the other hand, with a particular sensitivity to inelastic strain ($\gamma \to \alpha'$ phase transformation). Thermodynamic conditions of

DSA and plastic strain induced phase transformation are strictly linked to the so-called thermodynamic instability related to vanishing specific heat when the temperature approaches absolute zero. The DSA effect manifests itself at the macroscopic level by the so-called discontinuous plastic flow (serrated yielding), whereas the phase transformation converts the material from a homogeneous to heterogeneous two-phase continuum. Both types of material instability alternate in the vicinity of temperature T_1 (material parameter) that characterizes transition from screw dislocations to the edge dislocations mode. Finally, both phenomena are accompanied by nucleation and evolution of micro-damage fields, driven by inelastic strains that develop at very low temperatures.

The present paper is focused on constitutive description of FCC materials applied at very low temperatures. As an example, Fe-Cr-Ni austenitic stainless steels are commonly used to manufacture components of superconducting magnets and cryogenic transfer lines since they preserve ductility practically down to $0\,\mathrm{K}$. The constitutive description addresses all the three above listed phenomena driven by plastic strains at low temperatures: discontinuous (serrated) yielding, strain induced $\gamma \rightarrow \alpha'$ phase transformation and evolution of micro-damage. All of them are of dissipative nature and lead to irreversible processes in the material lattice. Even if the metastable stainless steels have been chosen in the present paper as a field of application of the constitutive description, the models presented in the course of the paper can be easily adopted to describe other materials used at cryogenic temperatures (like copper, copper and aluminium alloys, etc.). Their ductile behaviour down to $0\,\mathrm{K}$ implies evolution of plastic strain fields as soon as the stresses exceed the yield point characteristic of a given temperature.

Stainless steels (typically: grades 304L, 316L, 316LN) applied at low temperatures prove unstable both with respect to plastic flow and to $\gamma \rightarrow \alpha'$ phase transformation. Three distinct domains of the response of LSFE materials are identified for one of the most frequently applied materials: stainless steel 316LN (cf. Obst and Nyilas, 1991). Domain I corresponds to the temperature range below T_1 and to plastic flow instability called the discontinuous or serrated yielding. Domain II stretches between T_1 and M_d, the latter being the temperature above which the process of plastic strain induced $\gamma \rightarrow \alpha'$ phase transformation does not take place. Inside this domain the plastic flow is smooth and accompanied by transformation from the parent γ phase to the secondary α' phase. The phase transformation leads to a significant increase of the yield stress. Finally, domain III above the temperature M_d is characterized by smooth plastic flow and rather stable behaviour with respect to the

phase transformation. It is worth pointing out that the evolution of micro-damage occurs in all three domains and is driven by stable or unstable plastic flow. As all the above mentioned phenomena lead to irreversible degradation of lattice and can accelerate the process of material failure, a combined constitutive description is fundamental for correct prediction of the critical state of the material.

2. Kinetics of plastic strain induced phenomena at cryogenic temperatures

2.1. Kinetics of discontinuous (serrated) yielding (domain I)

At very low temperatures (below T_0 or T_1) and for sufficiently high strain rate, discontinuous plastic flow (serrated yielding) is observed. The main feature of serrated yielding consists in frequent abrupt drops of stress as a function of strain during monotonic loading. The mechanism of discontinuous yielding is related to formation of dislocation pile-ups at strong obstacles such as the Lomer-Cottrell locks during the strain hardening process. The back stresses of the piled-up groups block motion of newly created dislocations. The local shear stress at the head of dislocation pile-up, proportional to the number of dislocations in the pile-up, may reach the level of cohesive strength and the Lomer-Cottrell lock may collapse by becoming a glissile dislocation. This process takes place below the temperature T_0 or T_1, where the dislocations have a predominant edge character and cannot leave the pile-up by cross-slip.

Such a local catastrophic event can trigger similar effects in other groups of dislocations. Thus, the final result is massive and has a collective character. At low temperatures, where very high stresses are expected, this avalanche-like process is followed by spontaneous generation of dislocations by the rapidly increasing number of sources. This – in turn – leads to load drops observed in the stress-strain curve. During a tensile test at low temperature, the avalanche-like barrier crossing by dislocation pile-ups is manifested by acoustic effects of "dry" sounds emitted by the specimen. Periodic vibrations induced by a series of catastrophic events can be investigated by an analytical method related to impacting mechanical systems (cf. Palej and Nizioł, 1986). Each "serration" (sudden drop of stress as a function of time) is accompanied by a considerable increase of temperature, related to dissipation of plastic power and "thermodynamic instability" described in the previous section. A typical stress-strain

curve for the material that exhibits discontinuous yielding (stainless steel 316L at 4.2 K) is illustrated in Fig. 1a. Every "spike" in the stress-strain diagram shows a similar pattern: after the initial elastic process (stage 1), smooth plastic flow occurs (stage 2) until the abrupt drop of stress (stage 3) and further relaxation (stage 4) take place (cf. Obst and Nyilas, 1998).
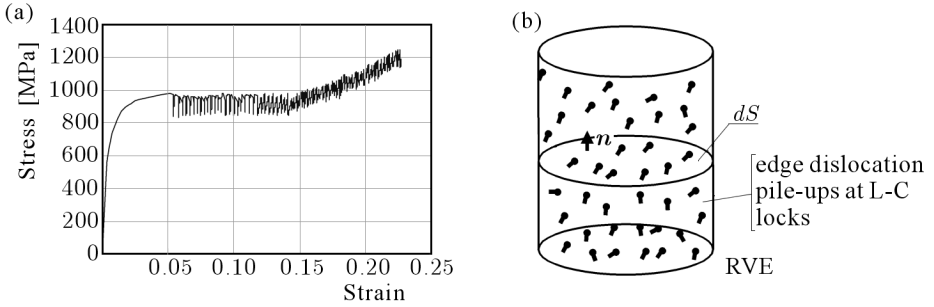

Fig. 1. (a) Serrated yielding in FCC metals (316L at 4.2 K). (b) RVE and dislocation groups localized at Lomer-Cottrell locks

No significant increase of temperature is observed during the smooth plastic flow. The temperature increases dramatically when the abrupt relaxation of stress begins. During the process of stress relaxation, the temperature rise induces a significant decrease of the yield point as the properties of FCC materials are highly temperature dependent. With increasing temperature, the dislocations become again more mobile and the further straining process occurs at much lower stress levels.

The main function that reflects the readiness of lattice with respect to discontinuous plastic flow is the cumulative volume of dislocation groups (located at the Lomer-Cottrell locks) per unit volume of lattice. This parameter will be called the volume fraction of dislocation groups and denoted by B

$$B = \frac{dV_B}{dV} \qquad 0 \leqslant B \leqslant 1 \tag{2.1}$$

where dV_B denotes the volume fraction occupied by dislocation groups and dV stands for the total volume. The RVE containing the dislocation groups is shown in Fig. 1b. It is assumed that the incremet of B strictly related to the increment of accumulated plastic strain (Odqvist parameter)

$$dp = \sqrt{\frac{2}{3}d\varepsilon^p : d\varepsilon^p} \tag{2.2}$$

Increasing intensity of the plastic flow generates more barriers for motion of the dislocations. Therefore, the following kinetic law of evolution for the volume fraction of the dislocation groups is postulated

$$\dot{B} = F_{LC}(T, \boldsymbol{\sigma})\dot{p}H(p - p_{LC}) \tag{2.3}$$

where F_{LC} is a function of temperature and the level of stress whereas p_{LC} represents a threshold above which the Lomer-Cottrell barriers massively develop. For an isothermal process and small variation of the flow stress, a simple linear representation is obtained

$$dB = F_{LC}dp \qquad p \geqslant p_{LC} \tag{2.4}$$

2.2. Kinetics of phase transformation and related phenomena (domain II)

The plastic strain induced $\gamma \rightarrow \alpha'$ phase transformation in metastable materials like stainless steels occurs in a wide range of temperatures below M_d. For instance, it can be easily activated at 77 K in liquid nitrogen. The process is controlled via the transformation kinetics, represented by the phase transformation curve. Kinetics of the $\gamma \rightarrow \alpha'$ phase transformation, developed by Olson and Cohen (1975) is reflected by a typical sigmoidal curve defining the evolution of the martensite content ξ as a function of the plastic strain. Under isothermal conditions and for a given strain rate, the classical sigmoidal curve has the form shown in Fig. 2b. At very low temperatures, the phase transformation process can be subdivided into three stages: low rate transformation below the threshold p_ξ (stage I), fast transformation with a high and nearly constant transformation rate (stage II) and asymptotically vanishing transformation with the rate decreasing to 0 and the volume fraction of martensite reaching a maximum ξ_L (stage III). If the plastic strain induced phase transformation occurs at very low temperatures (typically liquid helium 4.2 K or liquid nitrogen 77 K), then the steep part of the transformation curve (stage II) remains in the domain of relatively small strains (below 0.2). In this case, the constitutive modelling can be considerably simplified and stays within the scope of the classical rate-independent theory of plasticity.

A simplified evolution law for the volume fraction of martensite has been introduced for the linear part (II) of the sigmoidal curve by Garion and Skoczeń (2002)

$$\dot{\xi} = A(T, \dot{\boldsymbol{\varepsilon}}^p, \boldsymbol{\sigma})\dot{p}H((p - p_\xi)(\xi_L - \xi)) \tag{2.5}$$

where $\dot{p}$ denotes the rate of the accumulated plastic strain. Here, ξ denotes the volume fraction of martensite, $A(\dots)$ is a function of temperature, stress state
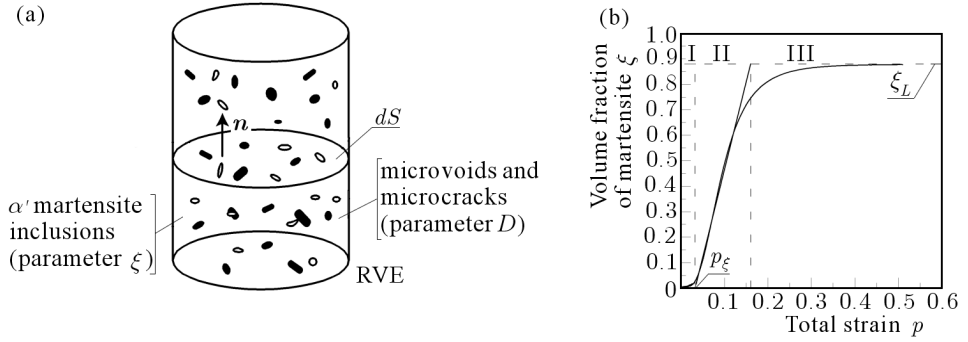
Fig. 2. (a) RVE with α'-martensite inclusions and micro-damage fields. (b) Volume fraction of α'-martensite versus accumulated plastic strain p

and strain rate, p_ξ denotes the accumulated plastic strain threshold (to trigger the formation of martensite), ξ_L stands for the martensite content limit and H represents the Heaviside function. The phase transformation from FCC to BCC lattice is driven by the accumulated plastic strain obtained by monotonic or cyclic straining at low temperatures. For an isothermal process and small variation of stress, again a simple linear representation is obtained

$$d\xi = Adp \qquad p \geqslant p_\xi \qquad \xi \leqslant \xi_L \tag{2.6}$$

2.3. Kinetics of micro-damage evolution (domains I, II and III)

The classical kinetic law of micro-damage evolution (Chaboche, 1988; Lemaitre, 1992) for isotropic and ductile damage postulates the following relation between the damage rate and the accumulated plastic strain rate

$$\dot{D} = \left(\frac{Y}{S}\right)^s \dot{p} H(p - p_D) \tag{2.7}$$

where Y stands for the strain energy density release rate, S denotes the strength energy of damage and p_D stands for the damage threshold. Here, D and Y form a pair of dual state variables, and S is a material modulus. The driving force of damage evolution is the accumulated plastic strain. In the case of anisotropic ductile damage, the damage parameter D (Fig. 2) is replaced by the damage tensor $\mathbf{D}$ (cf. Murakami, 1990) and the scalar function of the strain energy density release rate Y is replaced by the relevant tensor $\mathbf{Y}$ (cf. Lemaitre, 1992). Again, both $\mathbf{D}$ and $\mathbf{Y}$ form a pair of dual state variables.

In the present paper, it is assumed that the driving force of evolution of anisotropic ductile damage remains the accumulated plastic strain. The strength energy of damage S is replaced by the tensor $\mathbf{C}$, which defines material properties in the principal directions of damage. Furthermore, it is assumed that as soon as the damage threshold p_D has been reached, damage starts developing driven by the increase of the accumulated plastic strain p. However, the damage evolution is different along the principal directions described by the eigenvectors of the tensor $\mathbf{D}$. Thus, the kinetic law of damage evolution is postulated in the following form (cf. Garion and Skoczeń, 2003)

$$\dot{\mathbf{D}} = \mathbf{C}\mathbf{Y}\mathbf{C}^{\top}\dot{p}H(p - p_D) \tag{2.8}$$

which assures that the damage tensor is symmetric. In the direct notation, Eq. (2.8) is equivalent to

$$\dot{D}_{ij} = C_{ik}Y_{kl}C_{jl}\dot{p}H(p - p_D) \tag{2.9}$$

Here, the tensor $\mathbf{C}$ has been imposed on the tensor $\mathbf{Y}$ with respect to the index k, and the product has been again imposed on the tensor $\mathbf{C}^{\top}$ with respect to the index l. The tensor $\mathbf{C}$ is defined as follows

$$\mathbf{C} = \sum_{i=1}^{3} C_i \boldsymbol{n}_i \otimes \boldsymbol{n}_i \tag{2.10}$$

and can be classified as a symmetric tensor containing the material moduli. The kinetic law of damage evolution has been built as a direct extrapolation of the isotropic reference case. The isotropic conjugate damage variables, D and Y, can be obtained from the anisotropic state variables $\mathbf{D}$ and $\mathbf{Y}$ by the following operations

$$Y = \operatorname{tr}[\mathbf{Y}] \tag{2.11}$$

and, assuming that $\mathbf{C} = C\mathbf{I}$ for an isotropic material, the first invariant of the damage rate tensor reads

$$\dot{D} = \operatorname{tr}[\dot{\mathbf{D}}] = C^2 Y \dot{p} \tag{2.12}$$

which corresponds to the isotropic damage evolution law with $S = 1/C^2$. In the simple isotropic case and for $s = 1$, one obtains:

$$dD = \frac{Y}{S}dp \qquad p \geqslant p_D \tag{2.13}$$

3. RVE-based constitutive description of discontinuous yielding, $\gamma \to \alpha'$ phase transformation and micro-damage evolution

3.1. Discontinuous (serrated) yielding (domain I)

The discontinuous plastic flow reflects the dynamic strain ageing effect that occurs below the temperature T_0 or T_1. It has been explained (cf. Obst and Nyilas, 1991) by the mechanism of rapid formation of dislocation pile-ups at strong obstacles such as Lomer-Cottrell locks. The shear stress applied to the head of dislocation pile-up is multiplied by a factor proportional to the number of dislocations in the group. Simultaneously, the back stresses of dislocation groups block movement of new dislocations. As soon as the stress concentration at the leading edge is high enough, local catastrophic failure of the Lomer-Cottrell (LC) locks occurs and triggers the avalanche process that spreads over a larger portion of the material. Failure of LC locks leads to massive motion of released dislocations as well as spontaneous generation of dislocations by new sources, accompanied by a step-wise increase of the strain rate. The initially microscopic process becomes macroscopic and leads to load drops observed in the stress-strain curve. The local shear stress τ is accompanied by the amount of crystallographic slip, denoted by γ. Let us assume that the local dislocation density at a temperature T is denoted by ρ. The evolution of dislocation density with deformation is described by the following equation

$$\frac{d\rho}{d\gamma} = \frac{d\rho}{d\gamma}\Big|_{+} + \frac{d\rho}{d\gamma}\Big|_{-} \tag{3.1}$$

where the component denoted by "+" represents the rate of production of dislocations and the component denoted by "−" stands for the rate of annihilation of dislocations (cf. Bouquerel *et al.*, 2006). The production part is expressed by the formula

$$\frac{d\rho}{d\gamma}\Big|_{+} = \frac{1}{\lambda b} \tag{3.2}$$

where λ is the mean free path of dislocation and b denotes length of the Burgers vector. The annihilation part is given by the following relation

$$\frac{d\rho}{d\gamma}\Big|_{-} = -k_a \rho \tag{3.3}$$

where k_a represents the dislocation annihilation constant. The mean free path of dislocation obeys the following rule

$$\lambda = \frac{1}{\sum_i \lambda_i^{-1}} \tag{3.4}$$

with λ_i denoting the mean free path related to a specific type of obstacle. In the present paper, three types of obstacles will be taken into account: grain boundaries, dislocations and LC locks

$$\frac{1}{\lambda} = \frac{1}{d} + k_1\sqrt{\rho} + k_2\sqrt{B} \tag{3.5}$$

where d is the average grain size and k_1, k_2 are constants. Combining Eqs. (3.1) through (3.5), one obtains

$$\frac{d\rho}{d\gamma} = \frac{1}{db} + \frac{k_1}{b}\sqrt{\rho} + \frac{k_2}{b}\sqrt{B} - k_a\rho \tag{3.6}$$

Assuming the following relations for the macroscopic stress and strain

$$\sigma = M\tau \qquad \gamma = M\varepsilon \tag{3.7}$$

where M is the Taylor factor, and accepting that

$$\varepsilon \approx \varepsilon^p \tag{3.8}$$

the following formula can be derived

$$\frac{d\rho}{d\varepsilon^p} = M\left(\frac{1}{db} + \frac{k_1}{b}\sqrt{\rho} + \frac{k_2}{b}\sqrt{B} - k_a\rho\right) \tag{3.9}$$

Making reference to Eq. (2.3) and assuming that

$$F_{LC} = \text{const} \qquad \varepsilon^p \geqslant \varepsilon^p_{LC} \tag{3.10}$$

the volume fraction of dislocation groups reads

$$B = F_{LC}(\varepsilon^p - \varepsilon^p_{LC}) \tag{3.11}$$

Thus, the evolution of dislocation density can be expressed as

$$\frac{d\rho}{d\varepsilon^p} = M\left(\frac{1}{db} + \frac{k_1}{b}\sqrt{\rho} + \frac{k_2}{b}\sqrt{F_{LC}(\varepsilon^p - \varepsilon^p_{LC})} - k_a\rho\right) \tag{3.12}$$

The average shear stress in the lattice is composed of lattice friction and interaction between the dislocations

$$\tau = \tau_0 + \mu\alpha b\sqrt{\rho} \tag{3.13}$$

where μ is the shear modulus and α is the coefficient of dislocations interaction. The shear stress at the head of dislocation pile-up (stress concentration point) amounts to

$$\tau_e = \frac{\pi(1-\nu)}{\mu b}\lambda\tau^2 \tag{3.14}$$

and is a quadratic function of the average shear stress in the lattice. Here, the mean free path of dislocation can be interpreted as a distance between the source and the barrier.

The following criterion of avalanche-like failure of LC locks is postulated

$$B = B_{cr} \tag{3.15}$$

Thus, as soon as the volume fraction of dislocation groups reaches its critical value, the avalanche-like process is triggered and – at least theoretically – all the LC barriers are broken. The process of massive failure of LC locks results in an instantaneous increase of the strain rate

$$\dot{\varepsilon} = \dot{\varepsilon}_0 + \Delta\dot{\varepsilon}H[(\varepsilon - \varepsilon_1)(\varepsilon_2 - \varepsilon)] \tag{3.16}$$

where

$$\varepsilon_2 > \varepsilon_1 \qquad \Delta\varepsilon_s = \varepsilon_2 - \varepsilon_1 \tag{3.17}$$

denotes the amount of slip during the catastrophic failure of dislocation barriers. Assuming that the process is kinematically controlled, the following equation for relaxation of strains in the portions of material outside the slip zone can be derived

$$\varepsilon = \widetilde{\varepsilon} - \Delta\varepsilon_s \tag{3.18}$$

where $\widetilde{\varepsilon}$ is the value of macroscopic strain just before the catastrophic event. Strain relaxation results in the proportional elastic drop of stress (Fig. 3b)

$$\Delta\sigma = E\Delta\varepsilon_s \tag{3.19}$$

with the residual stress after unloading equal to

$$\sigma_r = \widetilde{\sigma} - E\Delta\varepsilon_s \tag{3.20}$$

where $\widetilde{\sigma}$ is the value of macroscopic stress just before the catastrophic slip.

During the massive failure of LC locks followed by fast motion of glissile dislocations in the lattice, a quantity of heat is produced. The heat quantity is a function of the plastic work and internal friction in the lattice when the abrupt slip occurs

$$\Delta Q = \eta(\Delta W^p + \Delta W^f) \tag{3.21}$$

Here, η denotes the relevant conversion factor. Following the curve of specific heat under constant volume and assuming that temperature remains above absolute zero, the following temperature increment occurs

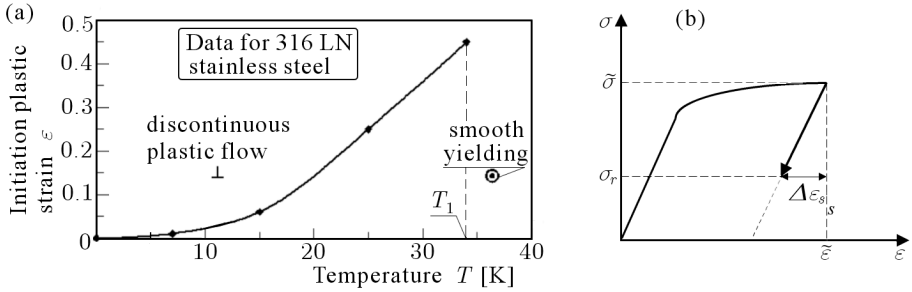$$\Delta T = \frac{\Delta Q}{mC_V(T)} \tag{3.22}$$

Fig. 3. (a) Initiation of discontinuous plastic flow. (b) Unloading outside the slip zone

This increase of temperature may even be of the order of 40-50 K. The temperature becomes a driving force in the process of stress relaxation (stage 4) down to a basic level determined by equilibrium conditions (cf. Zaiser and Haehner, 1997). The process of stress relaxation is described by the following set of equations

$$\sigma = \sigma_r + \Delta\sigma_T \qquad \frac{d}{dt}(\Delta\sigma_T) = \frac{1}{t_T}[(\sigma_\infty - \sigma_r) - \Delta\sigma_T] \qquad (3.23)$$

where σ_r, σ_∞ are the stress level after the catastrophic slip and the asymptotic strain rate sensitivity, respectively (stress level after the transients have died out), t_T denotes the characteristic time. The temperature relaxes towards a new steady state value inducing an additional evolution of the stress $\Delta\sigma_T$. After the process of stress relaxation has been completed, another dynamic strain ageing cycle begins.

The first two stages of the process reflect elastic-plastic loading under nearly isothermal conditions, corresponding to low excitation of the lattice. Under these circumstances (no thermal activation), the rate-independent plasticity can be applied, at least until the catastrophic failure of LC locks. Thus, the yield surface has the form

$$f_y(\boldsymbol{\sigma}, \mathbf{X}, R) = J_2(\boldsymbol{\sigma} - \mathbf{X}) - \sigma_y - R \qquad (3.24)$$

where

$$J_2(\boldsymbol{\sigma} - \mathbf{X}) = \sqrt{\frac{3}{2}(\mathbf{s} - \mathbf{X}) : (\mathbf{s} - \mathbf{X})} \qquad (3.25)$$

is the second invariant of the stress tensor. Here, $\mathbf{s}$, $\mathbf{X}$ denote the deviatoric stress and the back stress tensors, whereas σ_y, R are the yield stress and the

isotropic hardening variable, respectively. Furthermore, it is assumed that the continuum containing LC locks obeys the associated flow rule

$$d\boldsymbol{\varepsilon}^p = \frac{\partial f_y}{\partial \boldsymbol{\sigma}} d\lambda \tag{3.26}$$

with the yield function postulated as the potential of plasticity. The hardening model is represented by the following equations

$$d\mathbf{X} = \frac{2}{3} C_X d\boldsymbol{\varepsilon}^p \qquad\qquad dR = C_R dp \tag{3.27}$$

where C_X, C_R denote the kinematic and the isotropic hardening moduli, respectively. The evolution of parameter B can be computed from Eq. (2.3)

$$dB = F_{LC}(T, \boldsymbol{\sigma}) dp \tag{3.28}$$

It is assumed that in every loading/unloading "cycle" (single tooth in the stress-strain curve) the parameter B is accumulated from 0 to B_{cr}. As soon as condition (3.15) is fulfilled, the plastic flow instability (drop of stress) takes place.

3.2. Plastic strain induced $\gamma \to \alpha'$ phase transformation (domain II)

The RVE-based constitutive model presented in the paper describes behaviour of ductile materials in which the phase transformation occurs. The model is based on the following assumptions:

- two-phase continuum is composed of the austenitic matrix and martensite platelets represented by small Eshelby type ellipsoidal inclusions, randomly distributed and randomly oriented in the matrix,

- the austenitic matrix is elasto-plastic, whereas the inclusions show purely elastic response (the yield stress of martensite fraction is much higher than the yield stress of austenite),

- rate-independent plasticity is applied: it is assumed that the influence of the strain rate $\dot{\boldsymbol{\varepsilon}}^p$ is small in the range of temperatures 2-77 K, and the function $A(\ldots)$ depends on the temperature and stress state only,

- small strains are assumed: the accumulated plastic strain p does not exceed 0.2,

- mixed isotropic/kinematic hardening affected by the presence of martensite fraction is included,

- the two-phase material obeys the classical associated flow rule.

The constitutive model has been developed for a two-phase $(\gamma + \alpha')$ isotropic and ductile material (cf. Garion and Skoczeń, 2002). The kinetics of martensitic transformation has been already described in Section 2.2, Eq. (2.5). The general constitutive law includes plastic, thermal and transformation strains

$$\boldsymbol{\sigma} = \underline{\mathbf{E}} : (\boldsymbol{\varepsilon} - \boldsymbol{\varepsilon}^p - \boldsymbol{\varepsilon}^{th} - \xi \boldsymbol{\varepsilon}^{bs}) \tag{3.29}$$

where $\boldsymbol{\varepsilon}^p$ is the plastic strain tensor, $\boldsymbol{\varepsilon}^{bs} = (\Delta v \mathbf{I})/3$ denotes the free deformation called the bain strain expressed in terms of the relative volume change Δv, $\boldsymbol{\varepsilon}^{th}$ stands for the thermal strain tensor and $\underline{\mathbf{E}}$ is the fourth-rank elasticity tensor. It is assumed that the mesoscopic strain tensor $\boldsymbol{\varepsilon}^{bs}$ is obtained by integrating the microscopic eigen-strain tensor $\boldsymbol{\varepsilon}^{bs}_{\mu}$ over the RVE (cf. Garion *et al.*, 2006)

$$\boldsymbol{\varepsilon}^{bs} = \xi \frac{1}{3} \Delta v \mathbf{I} \tag{3.30}$$

For convenient description, it is assumed that the elastic stiffness tensor is expressed by

$$\underline{\mathbf{E}} = 3k\underline{\mathbf{J}} + 2\mu\underline{\mathbf{K}} \tag{3.31}$$

where the tensors $\underline{\mathbf{J}}$, $\underline{\mathbf{K}}$ are volumetric and deviatoric 4th rank projectors, respectively

$$\underline{\mathbf{J}} = \frac{1}{3}\mathbf{I} \otimes \mathbf{I} \qquad \underline{\mathbf{K}} = \underline{\mathbf{I}} - \underline{\mathbf{J}} \tag{3.32}$$

In the standard notation, the above equations are equivalent to

$$J_{ijkl} = \frac{1}{3}\delta_{ij}\delta_{kl} \qquad I_{ijkl} = \frac{1}{2}(\delta_{ik}\delta_{jl} + \delta_{il}\delta_{jk}) \tag{3.33}$$

Here, symbol $\otimes$ denotes the dyadic product, δ_{ij} is the Kronecker delta and k, μ denote the bulk and the shear moduli, respectively. The model of plastic flow is again based on the rate-independent plasticity, as indicated in Section 3.1, Eqs. (3.24)-(3.27). The hardening model is represented by the following equations

$$\dot{\mathbf{X}} = \frac{2}{3}C_X\dot{\boldsymbol{\varepsilon}}^p = \frac{2}{3}g(\xi)\dot{\boldsymbol{\varepsilon}}^p \qquad \dot{R} = C_R\dot{p} = f(\xi)\dot{p} \tag{3.34}$$

Since the hardening variables R and $\mathbf{X}$ are affected by the presence of martensite, the corresponding evolution laws are postulated in the following incremental form

$$d\mathbf{X} = d\mathbf{X}_a + d\mathbf{X}_{a+m} = \frac{2}{3}C(\xi)d\boldsymbol{\varepsilon}^p + G(\xi)d\boldsymbol{\varepsilon}^p = \frac{2}{3}g(\xi)d\boldsymbol{\varepsilon}^p$$

$$dR = f(\xi)dp \tag{3.35}$$

It is assumed that the back stress increment is composed of the classical term which corresponds to the behaviour of the austenitic phase $d\mathbf{X}_a$ in the presence of localized small inclusions, uniformly distributed and randomly oriented in the RVE and a term related to the combination of austenite and martensite via the homogenization algorithm $(d\mathbf{X}_{a+m})$. Furthermore, it is assumed that the mechanism of plastic flow at low temperatures is based on motion of dislocations in the lattice. If massive motion of dislocations occurs, they are stopped by the martensite inclusions and the corresponding local stress fields (Fig. 4a).
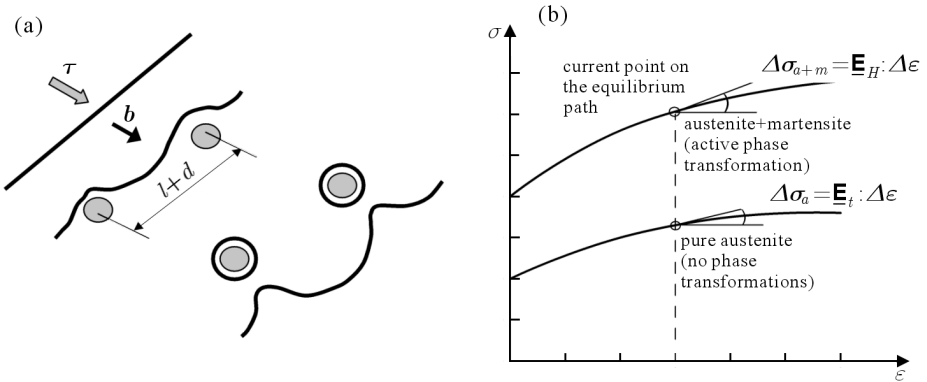

Fig. 4. (a) Interaction between dislocation and inclusions – the Orowan mechanism. (b) The principle of homogenization based on the local tangent stiffness moduli

The principal components that constitute the two-phase material model are the elasto-plastic matrix (austenite) and the highly localized elastic inclusions (martensite platelets). The linear kinematic hardening law is applied to model the plastic behaviour of pure austenite

$$dX_{a0} = \frac{2}{3}C_0 d\varepsilon^p \qquad (3.36)$$

where C_0 is the hardening modulus of the original non-transformed purely austenitic phase. For the two-phase transformed material, the hardening modulus C_0 is replaced by the modulus C that is higher than C_0 because of the interactions between the dislocations in the austenite and martensite inclusions

$$C = C_0 \varphi(\xi) \qquad \text{for} \ \ 0 \leqslant \xi \leqslant \xi_L$$

$$\varphi(0) = 1$$

$$(3.37)$$

It can be easily shown (cf. Skoczeń, 2007) that the shear stress necessary for dislocation to pass across two inclusions of the average size d, separated by the distance l, depends roughly linearly on the volume fraction of martensite ξ

$$\tau_p = \frac{\mu b}{d} \sqrt[3]{\frac{6\xi_0}{\pi}} \left(1 + \frac{\xi - \xi_0}{3\xi_0}\right) \tag{3.38}$$

where μ denotes the shear modulus of austenite, b is the length of the Burgers vector and ξ_0 stands for the initial volume fraction of inclusions. Here, for the sake of simplicity, an assumption has been made that the average size of inclusions d is constant and much smaller than the distance between two inclusions $d \ll l$. In the light of Eq. (3.38), the function $\varphi(\xi)$ takes the linear form

$$\varphi(\xi) = h\xi + 1 \tag{3.39}$$

where h is a material-dependent parameter. The function $\varphi(\xi)$ can be interpreted as that part of the hardening process which corresponds to the increase in volume fraction of martensite, and an enhanced probability that the dislocation will stack on the inclusion. The back stress increment corresponding to the behaviour of austenite in the presence of highly localized martensite inclusions can be decomposed in the following way

$$d\mathbf{X}_a = d\mathbf{X}_{a0} + d\mathbf{X}_{a\xi} = \frac{2}{3}C_0 d\varepsilon^p + \frac{2}{3}C_0 h\xi d\varepsilon^p = \frac{2}{3}C(\xi)d\varepsilon^p \tag{3.40}$$

where $d\mathbf{X}_{a\xi}$ corresponds to the interactions between dislocations in the austenitic matrix and martensite inclusions.

The second contribution to the hardening model is based on the principle of homogenization applied on the step-by-step basis to the current linearized tangent stiffness moduli of the matrix and the inclusions (Fig. 4b). As the matrix (γ-phase) is elastic-plastic, the relevant local linearized tangent stiffness tensor is derived. The inclusions are assumed to be ellipsoidal in shape and elastic, therefore, the elastic tangent stiffness is applied. The process of step-by-step homogenization based on the local tangent stiffness moduli follows the concept introduced by Hill (1965).

For the pure austenitic phase, a linearization of the stress/strain relations in the vicinity of the current state is expressed by

$$\Delta\boldsymbol{\sigma}_a = \underline{\mathbf{E}}_t : \Delta\varepsilon \tag{3.41}$$

where $\underline{\mathbf{E}}_t$ is the tangent stiffness tensor. A similar principle can be applied to a two-phase continuum. However, the tangent stiffness tensor is obtained by

the homogenization process

$$\Delta\boldsymbol{\sigma}_{a+m} = \underline{\mathbf{E}}_H : \Delta\varepsilon \tag{3.42}$$

The additional hardening increment induced by the presence of martensite is given by

$$\Delta\boldsymbol{\sigma} = \Delta\boldsymbol{\sigma}_{a+m} - \Delta\boldsymbol{\sigma}_a = (\underline{\mathbf{E}}_H - \underline{\mathbf{E}}_t) : \Delta\varepsilon \tag{3.43}$$

Here, the same "trial" strain increment has been assumed for pure austenite and for the homogenized two-phase continuum in order to compute the macroscopic stress response in the case of a strain controlled process. In the present paper, mainly the kinematically controlled $\gamma \to \alpha'$ phase transformation processes is analysed. The local linearized stiffness of austenite can be described by the following tangent stiffness tensor

$$\underline{\mathbf{E}}_{ta} = 3k_{ta}\underline{\mathbf{J}} + 2\mu_{ta}\underline{\mathbf{K}} \tag{3.44}$$

where

$$\mu_{ta} = \frac{E_t}{2(1+\nu)} \qquad k_{ta} = \frac{E_t}{3(1-2\nu)} \qquad E_t = \frac{EC}{E+C} \tag{3.45}$$

As the tangent operator for plastically active processes contains a dyadic square product of the vector normal to the yield surface in the stress space which makes the operator anisotropic, a linearization based on the quasi-isotropic operator is particularly justified in the case when the absolute values of the principal stresses are close to each other. When compared to the matrix, the inclusions are isotropic and elastic (their yield point is much higher than for pure austenite) and the corresponding elastic stiffness tensor is given by

$$\underline{\mathbf{E}}_m = 3k_m\underline{\mathbf{J}} + 2\mu_m\underline{\mathbf{K}} \tag{3.46}$$

where

$$\mu_m = \frac{E}{2(1+\nu)} \qquad k_m = \frac{E}{3(1-2\nu)} \tag{3.47}$$

The inclusions are assumed ellipsoidal and uniformly distributed in the matrix. Application of the Mori Tanaka homogenization scheme (cf. Garion *et al.*, 2006) yields

$$\underline{\mathbf{E}}_H = \underline{\mathbf{E}}_{MT} = 3k_{MT}\underline{\mathbf{J}} + 2\mu_{MT}\underline{\mathbf{K}} \tag{3.48}$$

with $\underline{\mathbf{E}}_{MT}$ obtained from the following relation

$$[\underline{\mathbf{E}}_{MT} + \underline{\mathbf{E}}^*]^{-1} = \sum_{i=a,m} f_i[\underline{\mathbf{E}}_i + \underline{\mathbf{E}}^*]^{-1} \tag{3.49}$$

where f_i is the volume fraction of the component i and $\underline{\mathbf{E}}^*$ stands for the Hill influence tensor. It is assumed that the strain increment is mainly due to the plastic strains: $\Delta\varepsilon \cong \Delta\varepsilon^p$. Thus, Eq. (3.46) becomes

$$\Delta\boldsymbol{\sigma} = [\underline{\mathbf{E}}_{MT} - \underline{\mathbf{E}}_t] : \Delta\varepsilon^p \tag{3.50}$$

The plastic strains are represented by a deviatoric tensor, therefore

$$\underline{\mathbf{J}} : \Delta\varepsilon^p = \mathbf{0} \qquad \underline{\mathbf{K}} : \Delta\varepsilon^p = \Delta\varepsilon^p \tag{3.51}$$

Finally, the additional stress increment due to the presence of martensite in the austenitic matrix is equal to

$$\Delta\boldsymbol{\sigma} = 2(\mu_{MT} - \mu_{ta})\Delta\varepsilon^p \tag{3.52}$$

If pure kinematic hardening is considered, the evolution of the back stress for the two-phase continuum obeys the following equation

$$\Delta\mathbf{X}_{a+m} = \Delta\boldsymbol{\sigma} \tag{3.53}$$

or in the incremental form

$$d\mathbf{X}_{a+m} = 2(\mu_{MT} - \mu_{ta})d\varepsilon^p \tag{3.54}$$

On the other hand, if pure isotropic hardening is considered, the evolution of the hardening parameter is obtained by imposing a suitable norm on the stress tensor

$$\Delta R = \Delta R_{a+m} = \frac{2}{3}J_2(\Delta\boldsymbol{\sigma}) = \frac{2}{3}\sqrt{\frac{3}{2}\Delta\boldsymbol{\sigma} : \Delta\boldsymbol{\sigma}} = 2(\mu_{MT} - \mu_{ta})\Delta p \tag{3.55}$$

where $\Delta p = \sqrt{2(\Delta\varepsilon^p : \Delta\varepsilon^p)/3}$. In the incremental form, one obtains

$$dR = dR_{a+m} = 2(\mu_{MT} - \mu_{ta})dp \tag{3.56}$$

Thus, for a unidirectional process of monotonic loading, the stress increments corresponding to the same increment of plastic strain are identical both for the kinematic hardening and for the isotropic hardening models. This linearized approach to the evolution of isotropic hardening is replaced by a more general nonlinear formulation, suitable for a greater martensite content

$$dR = (R_\infty(\xi) - R)dp \tag{3.57}$$

where R_∞ is the parameter that defines the ultimate size of the yield surface

$$R_\infty(\xi) = 2(\mu_{MT} - \mu_{ta}) \tag{3.58}$$

Eq. (3.57) can be reduced to Eq. (3.56) in the vicinity of the initial state.

In order to establish a proportion between the kinematic and the isotropic hardening, the Baushinger parameter β has been introduced (after Życzkowski, 1981)

$$\beta = \frac{\sigma' + \sigma'^-}{2(\sigma' - \sigma_0)} \qquad 0 \leqslant \beta \leqslant 1 \tag{3.59}$$

where σ' denotes the stress level at unloading and σ'^- is the stress level corresponding to the reverse active process. The parameter varies between 0 for the isotropic hardening (no Bauschinger effect) and 1 for the kinematic hardening (perfect Bauschinger effect).

Finally, the mixed hardening is described by the following model

$$d\mathbf{X} = \frac{2}{3}C_X d\varepsilon^p = \frac{2}{3}[C(\xi) + 3\beta b(\xi)(\mu_{MT} - \mu_{ta})]d\varepsilon^p$$
$$dR = C_R dp = b(\xi)(1 - \beta)(R_\infty(\xi) - R)dp \tag{3.60}$$

The relaxation term $b(\xi) = 1 - \xi$ has been added in order to compensate for the assumption that the martensite inclusions are elastic, whereas – in reality – they behave in an elastic-plastic way. The process of phase transformation induced strain hardening stops when $\xi = 1$.

3.3. Evolution of micro-damage (domains I, II and III)

Let us assume that at a given point in the RVE (Fig. 2) a local set of unit base vectors $\boldsymbol{n}_i$, tangent to the principal directions, has been defined. The damage tensor is postulated in the following form (cf. Murakami, 1990)

$$\mathbf{D} = \sum_{i=1}^{3} D_i \boldsymbol{n}_i \otimes \boldsymbol{n}_i \tag{3.61}$$

where $\boldsymbol{n}_i$ stands for the base vector associated with the principal direction i, and D_i denotes the component of the damage tensor related to the direction i. It is defined by

$$D_i = \frac{dS_{D_{n_i}}}{dS_{\boldsymbol{n}_i}} \tag{3.62}$$

where $S_{D_{n_i}}$ is the area of damage in the section $S_{\boldsymbol{n}_i}$ represented by the normal $\boldsymbol{n}_i$. The effective stress $\widetilde{\boldsymbol{\sigma}}$ is supposed to obey the strain equivalence principle (cf. Lemaitre, 1992)

$$\widetilde{\boldsymbol{\sigma}} = \underline{\mathbf{E}} : \varepsilon^e \tag{3.63}$$

For ductile materials, with a limited production of transverse damage, the strain equivalence principle turns out to be a good approximation of the real behaviour and does not lead to major errors. The relation between the stress and the effective stress tensors is postulated in the following form

$$\boldsymbol{\sigma} = \frac{1}{2}[(\mathbf{I} - \mathbf{D})\widetilde{\boldsymbol{\sigma}} + \widetilde{\boldsymbol{\sigma}}(\mathbf{I} - \mathbf{D})] \tag{3.64}$$

with $\mathbf{I}$ being the identity tensor. The general relationship between the stress and the effective stress tensors reads

$$\widetilde{\boldsymbol{\sigma}} = \underline{\mathbf{M}}^{-1} : \boldsymbol{\sigma} \qquad \boldsymbol{\sigma} = \underline{\mathbf{M}} : \widetilde{\boldsymbol{\sigma}} \tag{3.65}$$

where $\underline{\mathbf{M}}$ stands for the symmetric damage effect tensor that depends on the damage state. and fulfils the conditions

$$M_{ijkl} = M_{jikl} = M_{klij} \tag{3.66}$$

In its general form, the damage effect tensor is expressed by

$$\underline{\mathbf{M}} = \frac{1}{4}[(\mathbf{I} - \mathbf{D})\underline{\otimes}\mathbf{I} + (\mathbf{I} - \mathbf{D})\overline{\otimes}\mathbf{I} + \mathbf{I}\underline{\otimes}(\mathbf{I} - \mathbf{D}) + \mathbf{I}\overline{\otimes}(\mathbf{I} - \mathbf{D})] = \tag{3.67}$$

$$= \frac{1}{2}\underline{\mathbf{I}} - \frac{1}{4}[\mathbf{D}\underline{\otimes}\mathbf{I} + \mathbf{D}\overline{\otimes}\mathbf{I} + \mathbf{I}\underline{\otimes}\mathbf{D} + \mathbf{I}\overline{\otimes}\mathbf{D}]$$

where $\mathbf{a} \otimes \mathbf{b} = a_{ij}b_{kl}$, $\mathbf{a}\underline{\otimes}\mathbf{b} = a_{ik}b_{jl}$, $\mathbf{a}\overline{\otimes}\mathbf{b} = a_{il}b_{jk}$ or in direct notation

$$M_{ijkl} = \frac{1}{2}(\delta_{ik}\delta_{jl} + \delta_{il}\delta_{jk}) - \frac{1}{4}(D_{ik}\delta_{jl} + D_{il}\delta_{jk} + \delta_{ik}D_{jl} + \delta_{il}D_{jk}) \tag{3.68}$$

The strain energy density release rate tensor is defined by

$$\mathbf{Y} = -\rho\frac{\partial\Psi}{\partial\mathbf{D}} \tag{3.69}$$

where the Helmholtz free energy state potential coupled to damage can be written in the following form

$$\Psi = \frac{1}{\rho}\left(\frac{1}{2}\varepsilon^e : \underline{\mathbf{M}} : \underline{\mathbf{E}} : \varepsilon^e\right) + \Psi_p \tag{3.70}$$

Here, Ψ_p is the plastic part that does not explicitly depend upon $\mathbf{D}$. Eqs. (3.69) and (3.70), combined together, lead to the following representation

$$\mathbf{Y} = \frac{1}{4}[\varepsilon^e(\underline{\mathbf{E}} : \varepsilon^e) + (\underline{\mathbf{E}} : \varepsilon^e)\varepsilon^e] \tag{3.71}$$

The potential of dissipation is postulated in the following form (cf. Garion, Skoczeń, 2003)

$$\Phi = \frac{1}{2}(\mathbf{CYC}^\top) : \mathbf{Y} \sqrt{\frac{(\widetilde{\mathbf{s}} - \widetilde{\mathbf{X}}) : \underline{\mathbf{L}} : (\widetilde{\mathbf{s}} - \widetilde{\mathbf{X}})}{(\widetilde{\mathbf{s}} - \widetilde{\mathbf{X}}) : (\widetilde{\mathbf{s}} - \widetilde{\mathbf{X}})}} \tag{3.72}$$

where $\widetilde{\mathbf{s}}$ denotes the effective deviatoric stress, $\mathbf{C}$ is the tensor of material properties and

$$\underline{\mathbf{L}}(\mathbf{D}) = \underline{\mathbf{M}}^{-1}(\mathbf{D})\underline{\mathbf{M}}^{-1}(\mathbf{D}) \tag{3.73}$$

or in the direct notation

$$L_{ijkl} = M_{ijmn}^{-1} M_{mnkl}^{-1} \tag{3.74}$$

Here, Φ is a quadratic function of the conjugate force $\mathbf{Y}$, and is related to the damage rate by

$$\dot{\mathbf{D}} = \dot{\lambda}\frac{\partial \Phi}{\partial \mathbf{Y}} \tag{3.75}$$

The kinetic law of damage evolution can be derived directly from the above equation

$$\dot{\mathbf{D}} = \mathbf{CYC}^\top \dot{p} H(p - p_D) \tag{3.76}$$

where p_D denotes the damage threshold and $\mathbf{C}$ represents the texture-induced anisotropy of damage. Finally, the anisotropic damage evolution law becomes a generalization of the classical isotropic damage theory.

The general constitutive law includes again plastic, thermal and transformation strains

$$\widetilde{\boldsymbol{\sigma}} = \underline{\mathbf{E}} : (\boldsymbol{\varepsilon} - \boldsymbol{\varepsilon}^p - \boldsymbol{\varepsilon}^{th} - \xi\boldsymbol{\varepsilon}^{bs}) \tag{3.77}$$

As the model is based on the rate-independent plasticity, the yield surface takes the form

$$f_y(\widetilde{\boldsymbol{\sigma}}, \widetilde{\mathbf{X}}, \widetilde{R}) = J_2(\widetilde{\boldsymbol{\sigma}} - \widetilde{\mathbf{X}}) - \sigma_y - \widetilde{R} \tag{3.78}$$

where

$$\widetilde{\mathbf{X}} = \underline{\mathbf{M}}^{-1} : \mathbf{X} \qquad \widetilde{R} = \frac{R}{1 - \sqrt{\mathbf{D} : \mathbf{D}}} \tag{3.79}$$

are the effective kinematic and isotropic hardening variables, respectively. As already stated, it is assumed that – in the case of phase transformation – the two-phase continuum obeys the associated flow rule

$$d\boldsymbol{\varepsilon}^p = \frac{\partial f_y(\widetilde{\boldsymbol{\sigma}}, \widetilde{\mathbf{X}}, \widetilde{R})}{\partial \widetilde{\boldsymbol{\sigma}}} d\lambda \tag{3.80}$$

Finally, the hardening model is represented by the following equations

$$d\widetilde{\mathbf{X}} = \frac{2}{3}C_X d\varepsilon^p = \frac{2}{3}g(\xi)d\varepsilon^p$$

$$d\widetilde{R} = C_R dp = f(\xi)dp$$

(3.81)

where $f(\xi)$, $g(\xi)$ were defined in the previous section.

4. Conclusions

The constitutive model presented in the paper results from identification of three fundamental phenomena that occur at very low temperatures in structural materials characterized by low stacking fault energy:

- dynamic strain ageing reflected by discontinuous (serrated) yielding,
- plastic strain induced transformation from the parent phase γ to the secondary phase α', characteristic of meta-stable materials,
- evolution of micro-damage (micro-voids and micro-cracks) reflected by the decreasing elasticity modulus in the course of deformation.

All the three phenomena lead to irreversible degradation of lattice and accelerate the process of material failure. Therefore, a combined constitutive description is fundamental for correct dimensioning of structures applied at very low temperatures like superconducting magnets or cryogenic systems (Skoczeń and Wróblewski, 2007; Egner and Skoczeń, 2007). The constitutive model takes into account the relevant thermodynamic background related to mechanisms of heat transport in weakly excited lattice at very low temperatures.

It is worth pointing out that the combined model is attractive in view of its simplicity and a relatively small number of parameters to be identified at cryogenic temperatures. The experiments carried out in liquid helium or liquid nitrogen are laborious, expensive and usually require complex cryogenic installations to maintain stable conditions (constant or variable temperature). Therefore, any justified simplification leading to reduction of the number of parameters to be determined is of great importance.

References

1. Bouquerel J., Verbeken K., de Cooman B.C., 2006, Microstructure-based model for the static mechanical behaviour of multiphase steels, *Acta Materialia*, **54**, 1443-1456

2. Chaboche J.L., 1988a, Continuum damage mechanics: Part I – General concepts, *Jour. Applied Mechanics*, **55**, 59-64

3. Chaboche J.L., 1988b, Continuum damage mechanics: Part II – Damage growth, crack initiation and crack growth, *Jour. Applied Mechanics*, **55**, 64-72

4. Garion C., Skoczeń B., 2002, Modeling of plastic strain induced martensitic transformation for cryogenic applications, *Journ. of Applied Mechanics*, **69**, 6, 755-762

5. Garion C., Skoczeń B., 2003, Combined model of strain induced phase transformation and orthotropic damage in ductile materials at cryogenic temperatures, *Int. Journ. Damage Mech.*, **12**, 4, 331-356

6. Garion C., Skoczeń B., Sgobba S., 2006, Constitutive modelling and identification of parameters of the plastic strain induced martensitic transformation in 316 L stainless steel at cryogenic temperatures, *Int. Journ. of Plasticity*, **22**, 7, 1234-1264

7. Egner H., Skoczeń B., 2007, Model of anisotropic damage in ductile materials at cryogenic temperatures, *Proc. Conf. Thermal Stresses TS'07*, Taiwan

8. Hill R., 1965, A self consistent mechanics of composite materials, *J. Mech. Phys. Solids* , **13**, 213-222

9. Lemaitre J., 1992, *A Course on Damage Mechanics*, Springer-Verlag, Berlin and New York

10. Mori T., Tanaka K., 1973, Average stress in matrix and average elastic energy of materials with misfitting inclusions, *Acta Metall. Mater.*, **21**, 571-574

11. Murakami S., 1990, A continuum mechanics theory of anisotropic damage, In: *Yielding, Damage, and Failure of Anisotropic Solids, Proceedings of the IUTAM/ICM Symposium*, EGF Publication 5, 465-482

12. Obst B., Nyilas A., 1991, Experimental evidence on the dislocation mechanism of serrated yielding in f.c.c. metals and alloys at low temperatures, *Materials Science and Engineering*, **A137**, 141-150

13. Obst B., Nyilas A., 1998, Time-resolved flow stress behavior of structural materials at low temperatures, *Advances in Cryogenic Engineering (Materials)*, **44**, Plenum Press, New York, 331-338

14. Olson G.B., Cohen M., 1975, Kinetics of strain-induced martensitic nucleation, *Metallurgical Transactions*, **6A**, 791-795

15. Palej R., Nizioł J., 1986, On a direct method of analyzing impacting mechanical systems, *J. of Sound and Vibration*, **108**, 2, 191-198

16. Skoczeń B., 2004, *Compensation Systems for Low Temperature Applications*, Springer-Verlag, Berlin, Heidelberg, New York

17. Skoczeń B., 2007, Functionally graded structural members obtained via the low temperatures strain induced phase transformation, *Int. Journ. Sol. Struct.*, **44**, 5182-5207

18. Skoczeń B., Wróblewski A., 2007, Thermo-mechanical stress and strain fields resulting from the plastic strain induced phase transformation at cryogenic temperatures, *Proc. Conf. Thermal Stresses TS'07*, Taiwan

19. Zaiser M., Haehner P., 1997, Oscillatory modes of plastic deformation: theoretical concepts, *Phys. Stat. Sol. B*, **199**, 267-330

20. Życzkowski M., 1981, *Combined Loadings in the Theory of Plasticity*, PWN – Polish Scientific Publishers, Warsaw, Poland

Opis konstytutywny zjawisk wywołanych odkształceniami plastycznymi w temperaturach kriogenicznych

Streszczenie

Materiały konstrukcyjne (metale lub ich stopy) o sieci krystalicznej regularnej ściennie centrowanej są często stosowane w temperaturach kriogenicznych (także w temperaturach bliskich absolutnego zera) z uwagi na bardzo dobre własności fizyczne i mechaniczne, a w szczególności wysoką plastyczność. Materiały te, charakteryzujące się z reguły niską energią błędu ułożenia, podlegają w niskich temperaturach trzem procesom: dynamicznemu starzeniu odkształceniowemu (które generuje nieciągłe płynięcie plastyczne), przemianie fazowej od struktury regularnej ściennie centrowanej do struktury regularnej przestrzennie centrowanej oraz ewolucji mikrouszkodzeń. Wszystkie te zjawiska prowadzą do nieodwracalnej degradacji sieci krystalicznej i szybszego zniszczenia materiału, dlatego budowa modelu konstytutywnego staje się nieodzownym elementem projektowania konstrukcji pracujących w temperaturach kriogenicznych. Model konstytutywny przedstawiony w artykule ujmuje wszystkie wyżej wymienione zjawiska, jak również termodynamikę procesów zachodzących w sieci krystalicznej w niskich temperaturach.